CORE
Metadata, citation and similar papers at core.ac.uk
Provided by Elsevier - Publisher Connector

Cell

The NeST Long ncRNA Controls Microbial Susceptibility and Epigenetic Activation of the Interferon-γ Locus

J. Antonio Gomez,[1] Orly L. Wapinski,[2] Yul W. Yang,[2] Jean-François Bureau,[3] Smita Gopinath,[1] Denise M. Monack,[1] Howard Y. Chang,[2] Michel Brahic,[1] and Karla Kirkegaard[1,*]
[1]Department of Microbiology and Immunology
[2]Program in Epithelial Biology, Howard Hughes Medical Institute
Stanford University School of Medicine, Stanford, CA 94305, USA
[3]Département de Virologie, Institut Pasteur, 75724 Paris Cedex 15, France
*Correspondence: karlak@stanford.edu
http://dx.doi.org/10.1016/j.cell.2013.01.015

SUMMARY

Long noncoding RNAs (lncRNAs) are increasingly appreciated as regulators of cell-specific gene expression. Here, an enhancer-like lncRNA termed NeST (*ne*ttoie *S*almonella pas *T*heiler's [cleanup Salmonella not Theiler's]) is shown to be causal for all phenotypes conferred by murine viral susceptibility locus *Tmevp3*. This locus was defined by crosses between SJL/J and B10.S mice and contains several candidate genes, including NeST. The SJL/J-derived locus confers higher lncRNA expression, increased interferon-γ (IFN-γ) abundance in activated $CD8^+$ T cells, increased Theiler's virus persistence, and decreased *Salmonella enterica* pathogenesis. Transgenic expression of NeST lncRNA alone was sufficient to confer all phenotypes of the SJL/J locus. NeST RNA was found to bind WDR5, a component of the histone H3 lysine 4 methyltransferase complex, and to alter histone 3 methylation at the IFN-γ locus. Thus, this lncRNA regulates epigenetic marking of IFN-γ-encoding chromatin, expression of IFN-γ, and susceptibility to a viral and a bacterial pathogen.

INTRODUCTION

Bioinformatic analysis of the chromatin marks in intergenic DNA regions and of expressed sequence tags (ESTs) predicts the existence of more than 5,000 long noncoding RNA (lncRNA) genes in the human genome (Guttman et al., 2009; Khalil et al., 2009; Qureshi et al., 2010). However, it is currently unknown how many of these RNAs are functional. In a few well-studied cases, such as *AIR*, *XIST*, and *HOTAIR*, lncRNAs have been shown to operate at the transcriptional level by binding to proteins in histone-modifying complexes and targeting them to particular genes (Chu et al., 2011; Jeon and Lee, 2011; Nagano et al., 2008; Wang and Chang, 2011). A role for lncRNAs in mammalian susceptibility to infection or the immune response to pathogens has not been previously described.

NeST, formally known as *Tmevpg1*, is an lncRNA gene located adjacent to the interferon (IFN)-γ-encoding gene in both mice (*Ifng*) and humans (*IFNG*). *NeST* was originally identified as a candidate gene in a susceptibility locus for Theiler's virus (NeST stands for *ne*ttoie *S*almonella pas *T*heiler's [cleanup Salmonella not Theiler's]). In both mouse and human genomes, NeST RNA is encoded on the DNA strand opposite to that coding for IFN-γ, and the two genes are transcribed convergently (Figure 1A). In the mouse, NeST RNA contains six exons spread over a 45 kb region (Vigneau et al., 2001, 2003). The most abundant splice variant is 914 nt long, is expressed in $CD4^+$ T cells, $CD8^+$ T cells, and natural killer cells, and contains no AUG codons in translational contexts that appear functional. The orientation and location of human *NEST* are conserved, but the primary transcript encompasses the opposite strand of the entire *IFNG* gene (Figure 1A).

Theiler's virus, a picornavirus, is a natural pathogen of mice. The ability of inbred mice to clear Theiler's infection varies greatly from strain to strain, and, because the phenotype can be conferred by bone marrow transfer (Aubagnac et al., 2002; Brahic et al., 2005; Vigneau et al., 2003), is likely to result from different immune responses to the pathogen. A major effect is conferred by the *H2* locus. Two additional loci that affect Theiler's virus clearance were mapped by crosses between $H2^s$-bearing SJL/J and B10.S mice. Whereas B10.S mice can clear the virus, SJL/J mice become persistently infected and develop demyelinating lesions similar to those observed in human multiple sclerosis (Aubagnac et al., 2002; Bureau et al., 1993).

One of these loci, *Tmevp3* (*Theiler's murine encephalitis virus persistence 3*; Figure 1B), was mapped to a 550 kb interval on murine chromosome 10 (Levillayer et al., 2007). Congenic mouse lines were developed by crossing SJL/J to B10.S and backcrossing to each parental line for 10 to 12 generations (Bihl et al., 1999; Bureau et al., 1993; Levillayer et al., 2007). The $B10.S.Tmevp3^{SJL/J}$ line is congenic with B10.S but contains the *Tmevp3* locus from SJL/J and is unable to clear persistent infections. Conversely, the $SJL/J.Tmevp3^{B10.S}$ line is congenic

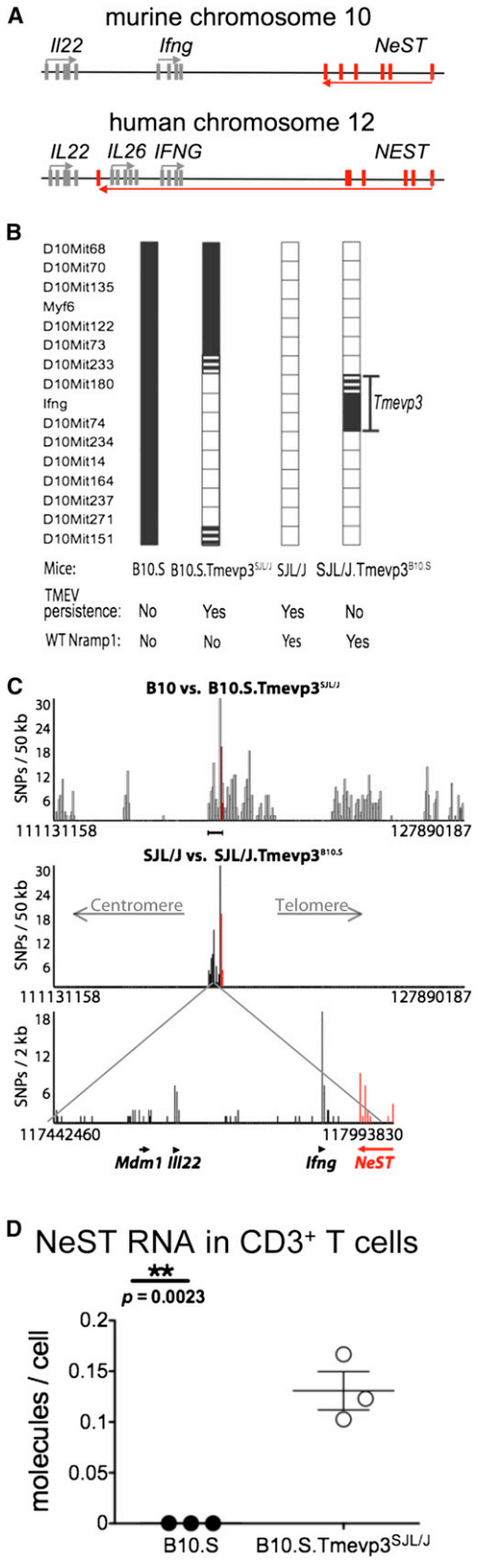

Figure 1. Genotypes of the Parental and Congenic Strains Used to Investigate NeST RNA and the *Tmevp3* Locus on Murine Chromosome 10

(A) Schematic of the *NeST*-encoding genes in mouse chromosome 10 and human chromosome 12. The bars represent exons, and arrows indicate the direction of transcription. *NeST* (previously termed *Tmevpg1*) is adjacent to both murine *Ifng* and human *IFNG* (Vigneau et al., 2003). The major transcript, shown in red, encodes six exons. In both mice and humans, the NeST and IFN-γ-encoding transcripts are convergently synthesized; in humans, the transcribed regions overlap.

(B) Diagram of the *Tmevp3* locus on murine chromosome 10, as defined by the differential ability to clear persistent infection by Theiler's virus observed between SJL/J and B10.S mice. The SJL/J.Tmevp3$^{B10.S}$ line (previously termed C2; Vigneau et al., 2003) is congenic with SJL/J except for the region shown, from microsatellite marker D10Mit74 to the interval between D10Mit180 and D10Mit233. The B10.S.Tmevp3$^{SJL/J}$ strain is congenic with B10.S except for the region shown, between the D10Mit151/D10Mit271 interval and the D10Mit233/D10Mit73 interval. The Theiler's virus (TMEV) persistence and clearance phenotypes and *Nramp1* alleles for all four strains are listed.

(C) Finer mapping of the polymorphic regions of the congenic lines. The x axis indicates the nucleotide number on mouse chromosome 10 (NCBI37/mm9). The introgressed region of SJL/J in B10.S.Tmevp3$^{SJL/J}$ is up to 1.6 × 10^7 bp (top), whereas the introgression in SJL/J.Tmevp3$^{B10.S}$ is approximately 5.5 × 10^5 bp (middle and bottom). Each bar displays the number of SNPs in the window size indicated. The most polymorphic region maps to the *Tmevp3* locus and coincides with the region of introgression in SJL/J.Tmevp3$^{B10.S}$; see Table S1 for lists of all genetic differences between the two *Tmepv3* alleles. The physical locations and direction of transcription of the murine *NeST*, *Ifng*, *Il22*, and *Mdm1* genes are indicated by arrows.

(D) NeST RNA expression in CD3$^+$ T cells. The abundance of NeST RNA in CD3$^+$ splenocytes from B10.S mice and B10.S.Tmevp3$^{SJL/J}$ was determined by preparing total cellular RNA and determining the amount of RNA per cell using qRT-PCR and standard curves of transcribed RNAs. The threshold of detection was 0.005 molecules of NeST RNA per cell. Mean values are shown with SE.

with SJL/J but contains the *Tmevp3* locus from B10.S and successfully clears infections. Analysis of SNPs in the smallest introgressed B10.S-derived region revealed a small number of polymorphic genes, including those that encode Mdm1 (Chang et al., 2008), the potent immune cytokines IL-22 and IFN-γ, and the lncRNA (Figure 1C).

Here, we show additional phenotypes associated with the *Tmevp3* locus. In addition to the failure to clear Theiler's virus, the SJL/J-derived alleles also confer both resistance to lethal infection with *Salmonella enterica* Typhimurium and inducible synthesis of IFN-γ in CD8$^+$ T cells. We show that NeST lncRNA is sufficient to confer these disparate phenotypes, demonstrating its crucial role in the host response to pathogens and illustrating an integral function for lncRNAs in immune regulation and susceptibility to infectious disease.

RESULTS

Mapping the Tmevp3 Locus of Mouse Chromosome 10

To refine the borders of the *Tmevp3* locus, we utilized the JAX mouse diversity genotyping array, which employs 623,124 SNPs and 916,269 invariant genomic probes. We also sequenced complementary DNAs (cDNAs) encoding interleukin-22 (IL-22), IFN-γ, and NeST RNA from SJL/J and B10.S mice, and added these findings to microarray results from the

Jackson Laboratory (Bar Harbor, ME; Figure 1C) and the list of known polymorphisms in the locus (Table S1 available online). Our results corroborated the presence of a unique introgressed region that contained the previously mapped *Tmevp3* locus, and allowed us to refine its boundaries. The maximum sizes of the introgressed regions were 16 × 10^6 bp and 550 × 10^3 bp, respectively, for the B10.S.Tmevp3$^{SJL/J}$ and SJL/J.Tmevp3$^{B10.S}$ congenic lines (Figure 1C).

These analyses identified *Il22*, *Ifng*, and *NeST* as the most likely candidates for the gene or genes responsible for the *Tmevp3* locus phenotypes by virtue of their polymorphic character and their known expression patterns. In Figure 1C, the top and middle bar graphs represent the number of SNPs in a series of nonoverlapping 50 kb window regions. The regions of densest polymorphism between the congenic and parental lines can be seen in more detail in the bottom part of Figure 1C. The product of *Mdm1* is expressed predominantly in the retina (Chang et al., 2008), making it an unlikely candidate. The three most polymorphic genes are *Ifng*, *NeST*, and *Il22*. The polymorphisms corresponding to *NeST* are shown in red and all polymorphisms in the locus are listed in Table S1. We were especially interested in the lncRNA because of its potential novelty. As shown in Figure 1D, CD3$^+$ T cells from B10.S.*Tmevp3*$^{SJL/J}$ mice displayed significantly higher amounts of NeST RNA than did those from B10.S mice. This result differs from that reported by Vigneau et al. (2003), possibly due to differences in the T cell preparations used or the use of saturating RT-PCR methods in the previous study. Here, quantitative RT-PCR (qRT-PCR), the use of standard curves, and comparisons of RNA abundances from identical numbers of cells showed repeatedly that splenocytes from mice with an SJL/J-derived *Tmevp3* allele accumulated substantially more NeST RNA than those from mice with a B10.S-derived *Tmevp3* allele. Even so, the amount of NeST RNA that accumulated in total CD3$^+$ T cells was, on average, only 0.15 molecules per cell (Figure 1D). It is known that many lncRNAs are present at similarly low amounts but still are sufficient to cause epigenetic changes that are then self-propagating (reviewed in Guttman and Rinn, 2012). It is also possible that NeST RNA is more abundant in a subset of the CD3$^+$ T cells. Indeed, a higher abundance of NeST RNA was observed in CD8$^+$ T cells (Figure 3B) than in total CD3$^+$ T cells (Figure 1D).

Additional Pathogen Phenotypes for the Tmevp3 Locus

To determine whether *Tmevp3* polymorphisms affected the outcome of another infection, we monitored their effects on the pathogenesis of *Salmonella enterica* Typhimurium, a pathogen that, like Theiler's virus, grows in macrophages (Monack et al., 2004; Rossi et al., 1997) and is extremely sensitive to IFN-γ and CD8$^+$ T cell control (Foster et al., 2005; Rodriguez et al., 2003). We began by comparing SJL/J and SJL/J.Tmevp3$^{B10.S}$ mice because the size of the introgressed region was smaller in this pair than in the B10.S and B10.S.Tmevp3$^{SJL/J}$ pair (Figure 1B). Both SJL/J mice and SJL/J.Tmevp3$^{B10.S}$ mice are homozygous for the functional allele of *Nramp1*, which encodes an ion channel that facilitates clearance of *Salmonella* (Frehel et al., 2002). As expected, both strains were resistant to oral inoculation (Figure 2A). However, when subjected to the more-potent intraperitoneal inoculation, both groups were susceptible but the SJL/J.Tmevp3$^{B10.S}$ mice showed significantly more mortality (Figure 2B).

B10.S and B10.S.Tmevp3$^{SJL/J}$ mice carry the *Nramp1*$^{169Asp/169Asp}$ loss-of-function allele, which increases their susceptibility to *Salmonella* infection. When inoculated orally, B10.S mice displayed significantly more mortality than B10.S.Tmevp3$^{SJL/J}$ mice at several infectious dosages (Figure 2C). Intraperitoneal inoculation was rapidly lethal for both mouse strains (Figure 2D). The differences in phenotypes between SJL/J and SJL/J.Tmevp3$^{B10.S}$ and also between B10.S and B10.S.Tmevp3$^{SJL/J}$ mice strengthen the hypothesis that the *Tmevp3* polymorphisms initially discovered by analysis of Theiler's virus persistence have implications for general immune function. In subsequent experiments, we focused on B10.S and B10.S.Tmevp3$^{SJL/J}$ mice and *Salmonella* pathogenesis, given that oral infection is the natural route.

To determine whether the differences in phenotype resulted from different bacterial loads, we infected B10.S and B10.S.Tmevp3$^{SJL/J}$ mice and monitored the abundance of *S.* Typhimurium in spleen and feces. B10.S and B10.S.Tmevp3$^{SJL/J}$ mice were orally inoculated with 10^6 CFU and spleens were dissected 4, 9, and 14 days after inoculation. No significant differences in bacterial loads were observed in either spleen or feces at any time point (Figure 2E). Interestingly, by day 14, both the B10.S and B10.S.Tmevp3$^{SJL/J}$ mice had nearly resolved their infections even though mice from both groups continued to die. To test for differences in *Salmonella* growth in cultured macrophages, we infected bone-marrow-derived primary macrophages from B10.S and B10.S.Tmevp3$^{SJL/J}$ and measured the amounts of intracellular *Salmonella* at various times after infection. No significant differences in bacterial growth within cells were observed (Figure 2F). All of these data are consistent with the hypothesis that lethality is not due to the bacterial load per se, but rather to the inflammatory response to bacterial infection (Miao and Rajan, 2011; Pereira et al., 2011; Strowig et al., 2012). In fact, the SJL/J-derived *Tmevp3* locus also conferred increased resistance to the lethal inflammatory disease caused by lipopolysaccharide (LPS) injection (Figure S1).

Transgenic Expression of NeST RNA Reproduces the Phenotype Associated with the SJL/J Tmevp3 Allele

We hypothesized that NeST RNA could play a causal role in the phenotypes conferred by the *Tmevp3* locus. To address this issue, we developed B10.S transgenic mice that express either SJL/J- or B10.S-derived NeST RNA under the control of a promoter that directs constitutive expression in both CD4$^+$ and CD8$^+$ T cells (Figure 3A; Sawada et al., 1994). We obtained two transgenic mouse lines: B10.S.NeST$^{B10.S}$ and B10.S.NeST$^{SJL/J}$. To test whether the transgenes had inserted near the endogenous *Tmevp3* locus, we performed genetic crosses between the B10.S.NeST$^{B10.S}$ and the B10.S.NeST$^{SJL/J}$ transgenic mice and mice that bore neither marker. For both transgenic lines, the NeST transgenes and the endogenous locus showed no evidence of linkage (data not shown). Both transgenic NeST RNAs were expressed in CD8$^+$ T cells (Figure 3B),

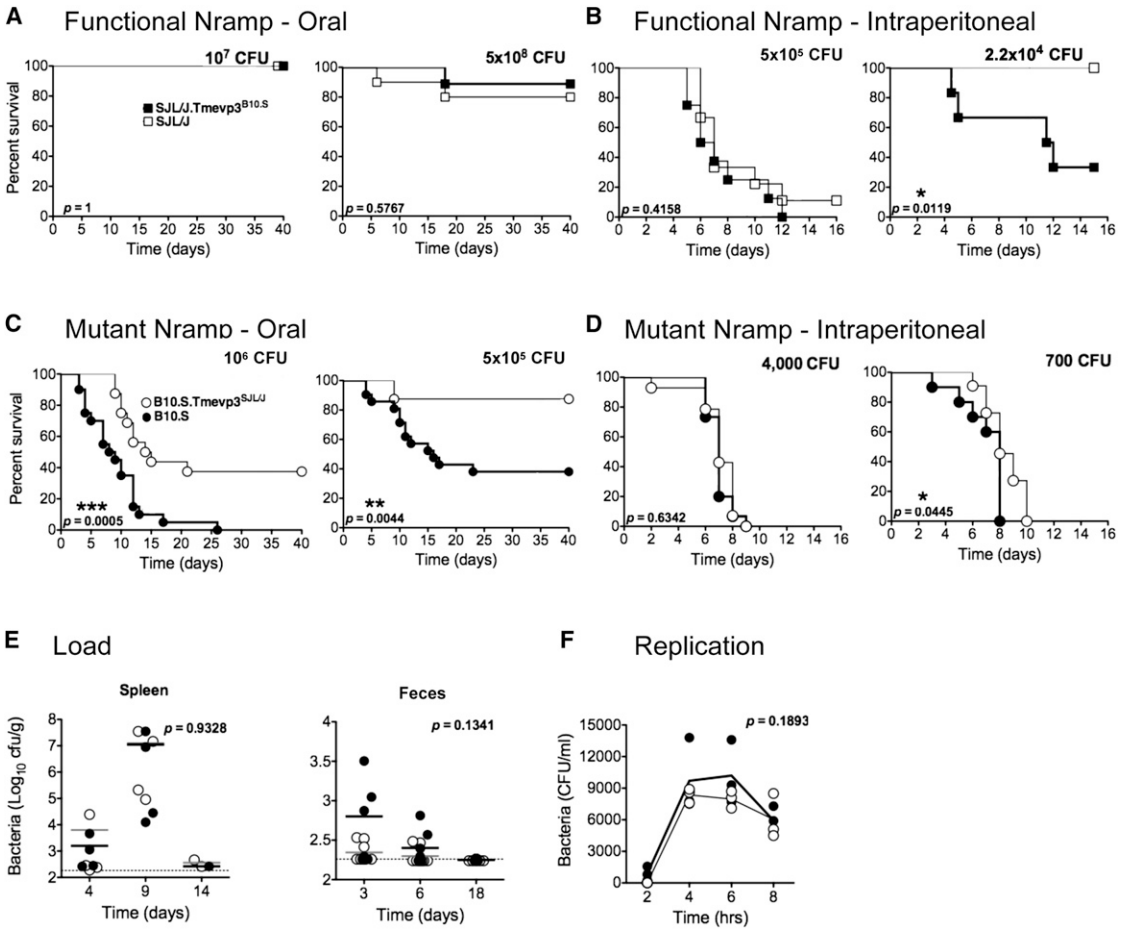

Figure 2. Effect of the *Tmevp3* Locus on *Salmonella* Pathogenesis

(A and B) Strains SJL/J and SJL/J.*Tmevp3*$^{B10.S}$ were inoculated via oral (A) and intraperitoneal (B) routes with *S. enterica* Typhimurium. The *Nramp1*$^{+/+}$ alleles expressed by SJL/J and SJL/J.*Tmevp3*$^{B10.S}$ mice render them relatively resistant to *Salmonella* infection.

(C and D) Strains B10.S and B10.S.Tmevp3$^{SJL/J}$ were also inoculated via oral (C) and intraperitoneal (D) routes with *S. enterica* Typhimurium at the dosages indicated and mortality was monitored. The *Nramp1*$^{169Asp/169Asp}$ alleles render these mice highly sensitive to *Salmonella* pathogenesis. In both backgrounds, the SJL/J allele of the *Tmevp3* locus reduced mortality after oral inoculation. Statistical significance was determined by the log rank test.

(E) B10.S and B10.S.Tmevp3$^{SJL/J}$ were orally inoculated with *S.* Typhimurium at 10^6 CFU/mouse. Bacteria were monitored in spleen and feces at the indicated days.

(F) Intracellular bacterial growth was monitored ex vivo in bone-marrow-derived macrophages from B10.S and B10.S.Tmevp3$^{SJL/J}$ mice. Lines represent the mean of triplicate experiments, and statistical significance was determined using Student's t test.

See also Figure S1.

although at different amounts. The B10.S NeST transgene was expressed to an abundance similar to that of the endogenous *NeST* gene in the B10S.Tmevp3$^{SJL/J}$ line, whereas the SJL/J-derived transgene accumulated to much greater abundance (Figure 3B).

To test whether the transgenic RNAs conferred protection against *Salmonella* pathogenesis, we inoculated B10.S mice, B10.S mice congenic at the *Tmevp3* locus, and B10.S mice transgenic for each NeST allele orally with *Salmonella*. Mice that expressed the NeST B10.S transgene completely recapitulated the *Tmevp3*$^{SJl/J}$ survival phenotype (Figure 3C). Mice that expressed the SJL/J NeST transgene also showed protection. These findings demonstrate that NeST RNA can function in *trans* to reduce *Salmonella* pathogenesis.

Transgenic NeST RNA Expression Prevents Clearance of Theiler's Virus

To test the role of NeST RNA in Theiler's virus infection, the microbial susceptibility phenotype that led to its discovery, we inoculated B10.S, B10.S.Tmevp3$^{SJL/J}$, and B10.S.NeST$^{B10.S}$ transgenic mice by intracranial injection. Viral loads in the spinal cord were determined seven and 67 days after inoculation. At seven days, all strains displayed comparable viral titers (Figure 4A), suggesting that NeST RNA plays little role during the acute phase of infection. However, 67 days after inoculation, infectious virus could only be recovered from mice that carried the NeST transgene or the B10.S.*Tmevp3* $^{SJL/J}$ locus (Figure 4B). The amounts of viral RNA in the spinal cords of the transgenic mice and the B10.S.Tmevp3$^{SJL/J}$ mice were orders of magnitude

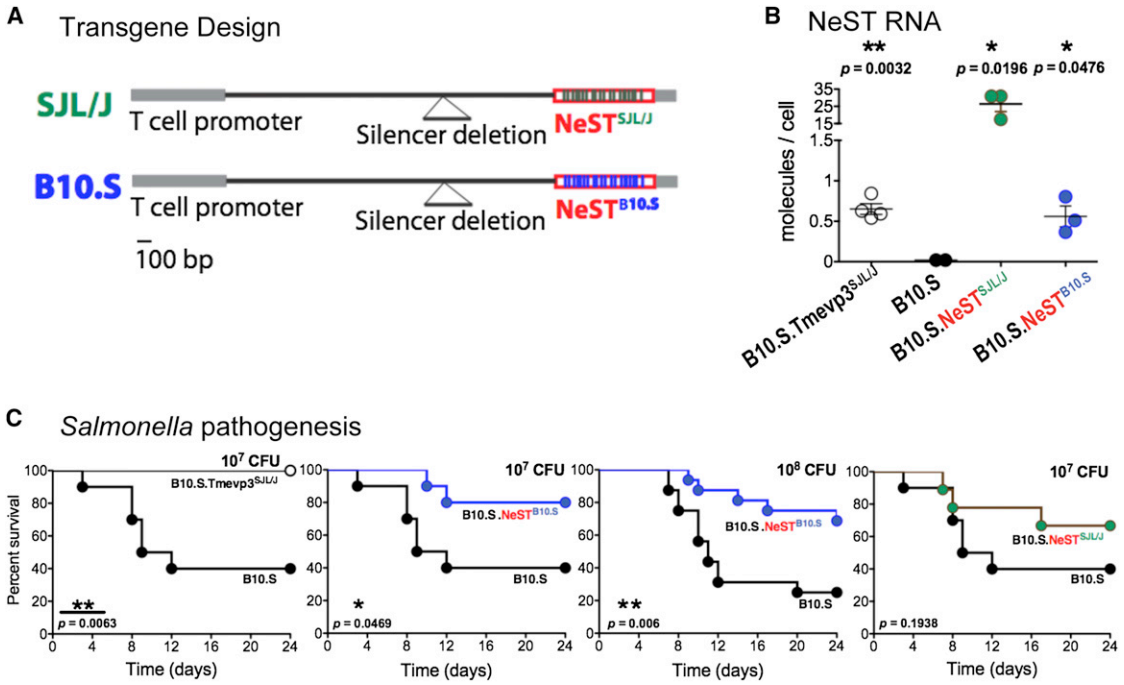

Figure 3. Effect of Transgenically Expressed NeST RNA on *Salmonella* Pathogenesis

(A) Schematic of transgenes introduced into B10.S mice. (S)JL/J NeST cDNA ([S]ea green) and (B)10.S NeST cDNA ([B]lue) were cloned downstream of a $CD4^+$ and $CD8^+$ T cell-specific promoter. The promoter-NeST transgene fragments were used to construct transgenic mouse lines in the B10.S background.

(B) The abundance of NeST RNA was measured in $CD8^+$ splenocytes from B10.S mice congenic for the SJL/J-derived *Tmevp3* locus (B10.S.Tmevp3$^{SJL/J}$), B10.S mice, B10.S mice containing the SJL/J NeST transgene (B10.S.NeST$^{SJL/J}$), and B10.S mice containing the B10.S NeST transgene (B10.S.NeST$^{B10.S}$). The amount of RNA per cell was determined using qRT-PCR; in vitro transcribed NeST RNA was used to construct standard curves. Mean values are shown with SE.

(C) B10.S, B10.S.Tmevp3$^{SJL/J}$, B10.S.NeST$^{SJL/J}$, and B10.S.NeST$^{B10.S}$ mice were orally inoculated with *S.* Typhimurium at the dosages indicated and mortality was monitored. All experiments with the 10^7 CFU/mouse were performed at the same time; the B10.S control is shown in these panels for clarity. Statistical significance was determined by the log rank test.

See also Figure S1.

higher than those found in the spinal cords of the nontransgenic B10.S parent (Figure 4C). Thus, the susceptibility to Theiler's virus persistence in spinal cord associated with the Tmevp3$^{SJL/J}$ allele was recapitulated by the expression of the NeST RNA transgene.

Effect of the Tmevp3 Locus on the Expression of IFN-γ by $CD8^+$ T Cells

Several enhancer-like lncRNAs are known to activate neighboring genes, as exemplified by HOTTIP and Jpx (Ørom et al., 2010; Tian et al., 2010; Wang et al., 2011). The physical proximity of *Il22* and *Ifng* to *NeST* inspired us to test for differences in expression of these two genes in $CD4^+$ and $CD8^+$ T cells from B10.S and B10.S.Tmevp3$^{SJL/J}$ mice. Isolated $CD4^+$ and $CD8^+$ T cells were cultured for 1 day, stimulated with phorbol 12-myristate 13-acetate (PMA) and ionomycin, and monitored for both cytokine secretion (Figures 5A and 5B) and intracellular RNA abundance (Figure S2). In $CD4^+$ T cells, ex vivo stimulation caused large but similar increases in the secretion of both cytokines in both B10.S and B10.S.Tmevp3$^{SJL/J}$ mice (Figure 5A). Similarly, the *Tmevp3* allele did not significantly affect the amounts of IL-22 secreted from $CD8^+$ T cells. However, whereas the amount of IFN-γ secreted from $CD8^+$ T cells derived from B10.S mice was barely detectible, IFN-γ secretion from B10.S.Tmevp3$^{SJL/J}$ mice was robust after stimulation (Figure 5B). The difference in IFN-γ production by $CD8^+$ T cells coincided with the amounts of IFN-γ RNA and NeST RNA (Figure S2B). These results show a strong correlation between the abundance of NeST RNA and IFN-γ RNA and the amount of IFN-γ protein in activated $CD8^+$ T cells.

Transgenic Expression of NeST Induces IFN-γ Synthesis in Activated $CD8^+$ T Cells

To determine whether the expression of NeST RNA alone could elicit the observed changes in IFN-γ expression in $CD8^+$ T cells, we monitored the abundance of the cytokine in $CD8^+$ T cells from B10.S, B10.S.NeST$^{SJL/J}$, and B10.S.NeST$^{B10.S}$ mice. As before, $CD8^+$ T cells from the parental B10.S mice accumulated very little cytokine after ex vivo stimulation (Figure 5C). However, the transgenic expression of either the B10.S or the SJL/J allele of NeST conferred the ability to induce IFN-γ secretion. Interestingly, the SJL/J-derived NeST RNA was less effective than the B10.S-derived RNA in mediating IFN-γ production, but both alleles caused statistically significant increases in IFN-γ expression upon $CD8^+$ T cell activation. Subsequent experiments were designed to investigate the mechanism of these effects.

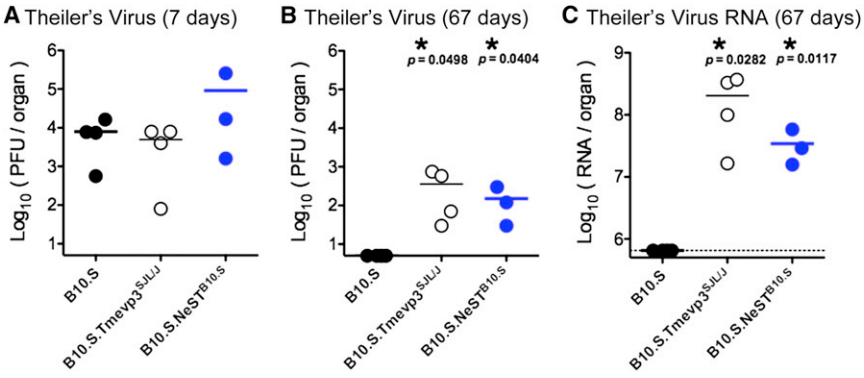

Figure 4. Effect of NeST RNA on Theiler's Virus Persistence

B10.S mice, B10.S mice congenic for the *Tmevp3* locus from SJL/J mice (B10.S.Tmevp3$^{SJL/J}$), and B10.S mice containing the B10.S NeST transgene (B10.S.NeST$^{B10.S}$) were inoculated by intracranial injections of 10^7 plaque-forming units (pfu) of Theiler's virus.

(A and B) Spinal cords were harvested at 7 days (A) and 57 days (B) postinoculation and viral load was measured by plaque assay on BHK-21 cell monolayers.

(C) The abundance of viral RNA in spinal cord from B10.S, B10.S.Tmevp3$^{SJL/J}$ and B10.S.NeST$^{B10.S}$ mice was determined by preparing total cellular RNA from homogenized tissue and determining the amount per gram of tissue using qRT-PCR. TMEV RNA was transcribed from cDNA-containing plasmid to construct standard curves. Means and SE are shown.

NeST Is a Nuclear lncRNA that Can Function in *trans* to Affect its Neighboring Locus

We hypothesized that, like several lncRNAs, NeST RNA affects IFN-γ accumulation at the transcriptional level by interacting with chromatin modification complexes. Consistent with this idea, most of the NeST RNA in either congenic or transgenic mice was found in the nuclear fraction of CD8$^+$ T cells, cofractionating with unspliced (but not with spliced) actin mRNA (Figure 6A).

The finding that two different transgenic NeST RNAs that were not genetically linked to the *Ifng* locus conferred the properties of the *Tmevp3*$^{SJL/J}$ locus to B10.S mice (Figures 3, 4, and 5) argues that this lncRNA can function in *trans*. To determine whether NeST RNA can indeed function in *trans* from its normal position of synthesis, we took advantage of the fact that NeST RNA is expressed in stimulated CD8$^+$ T cells of B10.S.Tmevp3$^{SJL/J}$ mice but not in CD8$^+$ T cells of B10.S mice (Figure 3B and S2B). We developed a PCR assay to distinguish between the SJL/J- and B10.S-derived IFN-γ alleles (Figure 6B). CD8$^+$ T cells from two heterozygous B10.S/B10.S.Tmevp3$^{SJL/J}$ mice were stimulated, RNA was extracted, and the allele from which the RNA was transcribed was determined from the RT-PCR shown in Figure 6B. Approximately equal amounts of IFN-γ mRNA from the B10.S and SJL/J alleles accumulated following stimulation (Figure 6C), arguing that the single functional NeST gene in the heterozygous mice could stimulate transcription from the *Ifng* genes on both chromosomes.

NeST RNA Binds to a Subunit of the MLL/SET1 H3K4 Methylase Complex and Increases Chromatin Modification at the Ifng Locus

If NeST RNA were to have a direct effect on the expression of IFN-γ, via chromatin modification, it should be an activating effect. Recently, a new class of enhancer-like lncRNAs was discovered (Ørom et al., 2010; Wang et al., 2011). Among these, HOTTIP lncRNA was found to bind WDR5 protein to recruit complexes that facilitate transcription (Wang et al., 2011). WDR5 is a core subunit of MLL1-4 and SET1A/1B complexes, which catalyze the methylation of histone H3 at lysine 4, a mark of active gene expression. To test whether NeST RNA physically interacts with WDR5, the epitope-tagged protein was coexpressed in combination with a variety of RNAs via transient transfection of 293T cells (Figure 7A). Extracts were then prepared and WDR5 protein was immunoprecipitated and tested for associated RNAs by qRT-PCR. HOTTIP served as a positive control, and both HOTAIR lncRNA and U1 nuclear RNA served as negative controls. Immunoprecipitation (IP) of WDR5 specifically retrieved both NeST RNAs and HOTTIP, but not U1 or HOTAIR RNAs (Figures 7A and 7B). The physical interaction between NeST and WDR5 raises the intriguing possibility that NeST may control H3K4 methylation at the *Ifng* locus.

To examine the contribution of NeST RNA to IFN-γ production during immune challenge, we used a well-characterized mouse model of sepsis: intraperitoneal injection of LPS. B10.S mice as well as B10.S.NeST$^{B10.S}$ and B10.S.NeST$^{SJL/J}$ transgenic mice were injected with LPS. By 6 hr postinjection, the presence of either transgenic NeST allele increased the amount of IFN-γ in splenic tissue compared with the B10.S control (Figure 7B). An increase in H3K4me3 occupancy at the *Ifng* locus preceded this increased IFN-γ synthesis by 2 hr (Figure 7B). Transgenic mice with the SJL/J-derived allele, which accumulate much more NeST RNA than those that express the B10.S allele (Figure 3B), showed a larger amount of IFN-γ-encoding DNA with H3K4me3 modifications (Figure 7B). Thus, increased NeST RNA abundance can result in more extensive H3K4me3 modification. Still, NeST RNA is extremely potent even at low abundance, either because the epigenetic effects persist in its absence or because activation of only a subset of cells is necessary for the observed phenotypes.

The high occupancy of H3K4me3 at the *Ifng* locus in the B10.S.NeST$^{SJL/J}$ transgenic mice allowed us to measure chromatin modification in isolated primary CD8$^+$ cells in the presence and absence of NeST RNA. Following activation of B10.S- and B10.S.NeST$^{SJL/J}$-derived CD8$^+$ T cells, we found that the presence of NeST$^{SJL/J}$ RNA caused an increase in H3K4me3 at the *Ifng* locus (Figure 7C). The NeST RNA-dependent increase in H3K4me3 activation in both total splenic cells and CD8$^+$ T cells strongly suggests that, via binding to WDR5, NeST RNA is

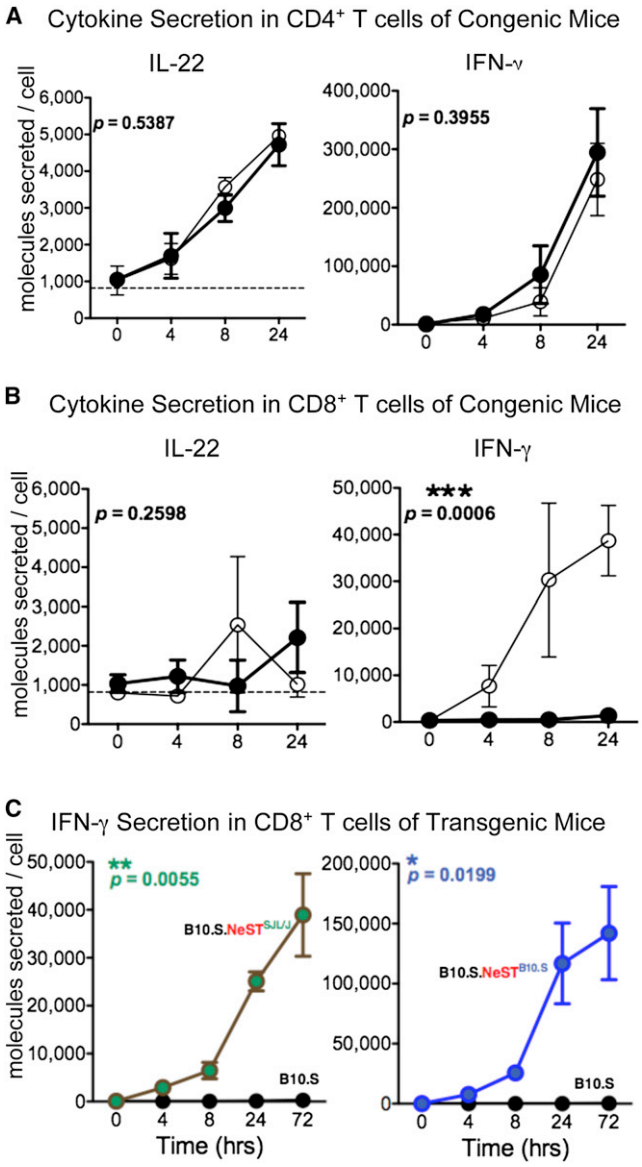

Figure 5. Effect of *Tmevp3* Locus and Transgenically Expressed NeST RNA on Cytokine Expression by T Cell Subsets

(A and B) Splenic (A) $CD4^+$ and (B) $CD8^+$ T cells were isolated from three B10.S (black circles) and three B10.S.Tmevp3$^{SJL/J}$ (white circles) mice and stimulated ex vivo with PMA and ionomycin. The abundance of IFN-γ and IL-22 protein secreted was determined by ELISA from supernatants collected at the indicated times. Means and SE are indicated for each time point. Statistical significance was determined using a two-way ANOVA test; asterisks denote values that differ significantly between T cells derived from B10.S and T cells derived from B10.S.Tmevp3$^{SJL/J}$ mice.

(C) Splenic $CD8^+$ T cells were isolated from B10.S (black), B10.S.NeST$^{SJL/J}$ (sea green), and B10.S.NeST$^{B10.S}$ (blue) mice and stimulated ex vivo with PMA and ionomycin. The abundance of secreted IFN-γ was determined by ELISA. Asterisks and p values refer to the comparisons between T cells derived from B10.S and T cells derived from each transgenic line.

See also Figure S2.

required to program an active chromatin state that confers inducibility to the *Ifng* gene.

DISCUSSION

In this work, we performed a genetic analysis of an lncRNA expressed in T cells. Mice that express NeST RNA, either in its natural chromosomal environment or by transgenic delivery, displayed increased resistance to *Salmonella*-induced pathogenesis but increased susceptibility to Theiler's virus persistence. These disparate effects illustrate the role of balanced polymorphisms in susceptibility to infectious disease (Dean et al., 2002; Liu et al., 1996; Williams et al., 2005; Wang et al., 2010; Cagliani et al., 2011). Genes of the immune system are under purifying selection by challenges from a plethora of pathogens, and mutations that protect against one microbe may increase susceptibility to another. In the case of autoimmunity, the rs2076530-G allele of *BTNL2*, a major histocompatibility complex (MHC) II-linked gene, confers increased susceptibility to rheumatoid arthritis and type 1 diabetes but decreased susceptibility to multiple sclerosis and autoimmune thyroiditis (Orozco et al., 2005; Sirota et al., 2009; Valentonyte et al., 2005).

A potential explanation for the disparate effects of NeST RNA on Theiler's virus persistence and *Salmonella* pathogenesis is that it alters the magnitude or timing of inflammatory responses. $CD8^+$ T cell populations are extremely heterogeneous (Davila et al., 2005; Joosten et al., 2007; Xystrakis et al., 2004); for example, the $CD8^+$ T_{reg} population is important in resolving inflammation and preventing autoimmunity (Frisullo et al., 2010; Sun et al., 2009; Trandem et al., 2011). Alternatively, NeST-dependent activation of basal inflammation could serve to attenuate subsequent inflammatory events. Finally, NeST RNA may have targets in addition to the *Ifng* gene that contribute to its apparently anti-inflammatory effect (Figure S2).

The fact that the effects of NeST can be conferred by transgenic expression from ectopic loci, and to *Ifng* alleles on both chromosomes when NeST is expressed heterozygously, argues that NeST function, even on the adjacent IFN-γ-encoding locus, can be provided in *trans*. Although many lncRNAs, such as Xist and HOTTIP, exert their function on neighboring genes exclusively in *cis*, *trans*-acting lncRNA function has precedent in HOTAIR, linc-p21, and Jpx lncRNAs (reviewed in Guttman and Rinn, 2012). Notably, *Jpx* is required to activate the expression of the adjacent *Xist* gene on the presumptive inactive X chromosome, and this activation can occur whether Jpx RNA is supplied in *cis* or *trans* (Tian et al., 2010). Thus, there is increasing recognition in the field that lncRNA regulation of nearby genes can occur by *trans*-acting mechanisms. The increased demands made on these lncRNAs for target specificity are currently under investigation.

In the vicinity of the *Ifng* locus, many of the distal regulatory elements map to regions now known to encode NeST (Sekimata et al., 2009). For example, acetylation of histone 4 (H4Ac), a mark of active transcription, has been observed in discrete regions surrounding *Ifng* in activated $CD4^+$ and $CD8^+$ T cells. One peak in particular, which correlates well with the differentiation of both $CD8^+$ and $CD4^+$ T cells (Chang and Aune, 2005; Zhou et al., 2004), is located 59 kb downstream of *Ifng* and coincides

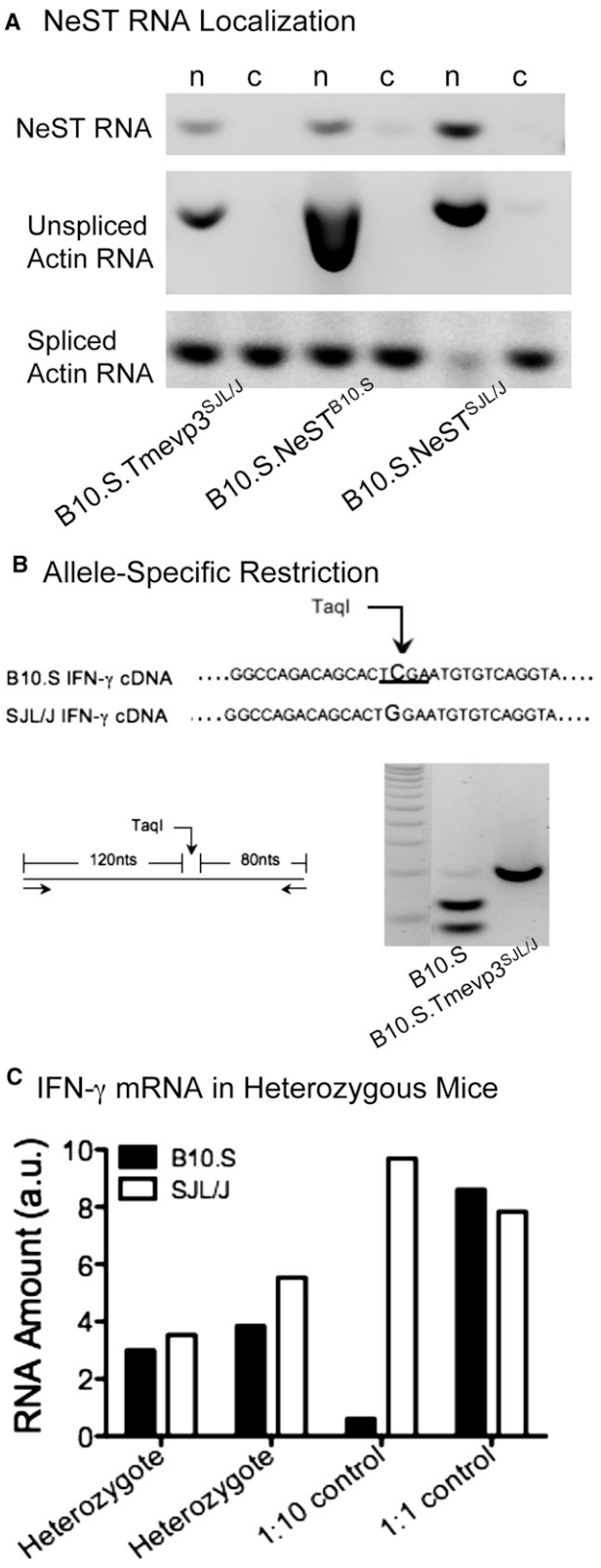

Figure 6. NeST RNA Localization and IFN-γ *trans* Activation

(A) Nuclear and cytoplasmic RNA from CD8$^+$ T cells from B10.S.Tmevp3$^{SJL/J}$, B10.S.NeST$^{B10.S}$, and B10.S.NeST$^{SJL/J}$ mice were fractionated by differential centrifugation (Huarte et al., 2010). NeST RNA, unspliced actin RNA (nuclear), and spliced actin RNA (cytoplasmic) from the nuclear and cytoplasmic fractions were assessed by RT-PCR and gel electrophoresis.

(B) Quantitation of expression ratios of IFN-γ mRNA from the B10.S and the B10.S.Tmevp3$^{SJL/J}$ alleles. A natural SNP in the IFN-γ mRNA (coordinate 117882772; see Table S1) was amplified by RT-PCR (top and left panel). cDNAs from B10.S and B10.S.Tmevp3$^{SJL/J}$ were subjected to a B10.S allele-specific TaqI restriction digest (bottom, left) and fragments were analyzed by gel electrophoresis.

(C) Splenic CD8$^+$ T cells were isolated from two B10.S × B10.S.Tmevp3$^{SJL/J}$ heterozygous mice and stimulated with PMA and ionomycin. The proportion of B10.S and B10.S.Tmevp3$^{SJL/J}$-derived IFN-γ mRNA was determined by densitometry of the allele-specific restriction fragments. Mixtures of in vitro transcribed RNAs at 1:10 and 1:1 ratios were used as controls.

with the sixth exon of NeST (Figure 1). Another noteworthy region that is critical for IFN-γ expression in CD4$^+$ T cells maps 66 kb downstream of murine *Ifng* and, in humans, 166 kb downstream of *IFNG*. This regulatory element is also located in the NeST gene. It contains a lineage-specific DNase I hypersensitive site found in Th1 but not Th2 CD4$^+$ T cells (Balasubramani et al., 2010). During lineage-specific induction of IFN-γ, the proteins CTCF, T-bet, and cohesin all localize to these sequences. Indeed, a recent study (Collier et al., 2012) related the expression of NeST RNA (*Tmevpg1*) to the expression of IFN-γ in CD4$^+$ T cells by a mechanism that depends on the simultaneous expression of T-bet. Simultaneous binding of cohesin, T-bet, and CTCF results in a complex three-dimensional conformation that is predicted to bring the NeST and IFN-γ coding regions into direct proximity (Hadjur et al., 2009; Ong and Corces, 2011; Sekimata et al., 2009).

Humans express an RNA species homologous to NeST that also appears to be noncoding and is transcribed adjacent to the *IFNG* locus from the opposite DNA strand. Interestingly, polymorphisms that correlate with autoimmune and inflammatory diseases such as rheumatoid arthritis, Crohn's disease, and multiple sclerosis have been found in the DNA sequence that encodes the first intron of the IFN-γ-encoding gene (Goris et al., 2002; Latiano et al., 2011; Silverberg et al., 2009); this DNA region also encodes the fifth intron of the overlapping NeST RNA-encoding gene. As they do in mice, variations in NeST RNA expression in humans could contribute to differences in T cell response and disease susceptibility. Whether and how disease-associated SNPs alter human NeST expression or function will be addressed in future studies.

Natural polymorphisms, both in humans and in animal models, can yield subtle quantitative allelic effects that are more difficult to study but are more relevant to human medicine than the effects of gene knockout or other loss-of-function genetic techniques. The discovery of NeST RNA was the result of classical forward genetics. Our analysis of NeST RNA was based on the conceptual framework that regions that are thought to be "intergenic" encode functional RNA elements. Many genome-wide association studies have also pointed to intergenic regions as heritable causes of human disease (Libioulle et al., 2007; Sotelo et al., 2010). This study establishes that some of these intergenic regions may encode functional lncRNAs that are critical for proper gene regulation. The promise of individualized medicine relies on our understanding of as many genetic polymorphisms

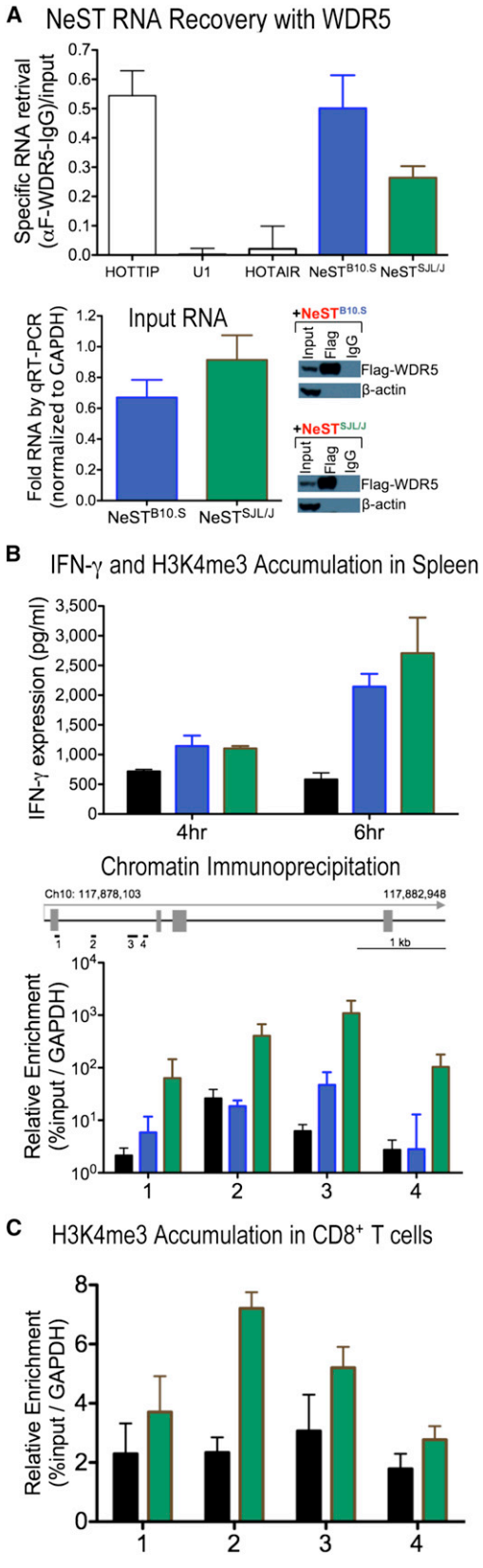

Figure 7. NeST RNA's Physical Association with WDR5 Protein and Effect on Histone 3 Lysine 4 Trimethylation at the *Ifng* Locus

(A) RNA preparations from 293T cells that were cotransfected with FLAG-tagged WDR5 cDNA and either B10.S-derived NeST cDNA (blue) or SJL/J-derived NeST cDNA (sea green) were analyzed after IP with either anti-FLAG antibodies or anti-immunoglobulin G (anti-igG) control antibodies. NeST RNA retrieval was determined by measuring RNA input levels normalized to glyceraldehyde 3-phosphate dehydrogenase (GAPDH; bottom left panel). Specific RNA retrieval was determined by subtracting NeST RNA retrieval with anti-igG antibodies from the retrieval with anti-FLAG antibodies, followed by normalization to the amount of input RNA. Immunoblot analysis (bottom right panel) confirmed FLAG-WDR5 expression following transfection and the specificity of the anti-FLAG and anti-igG antibodies.

(B) IFN-γ production and H3K4me3 occupancy in spleen following immune challenge. B10.S, B10.S.NeST$^{B10.S}$, and B10.S.NeST$^{SJL/J}$ mice were injected intraperitoneally with 50 μg of LPS, and spleens were dissected 4 and 6 hr later. The abundance of IFN-γ protein was determined by ELISA in tissue homogenates (top panel) and the occupancy of histone 3 lysine 4 trimethylation at the *Ifng* gene was determined by ChIP-qPCR analysis (bottom panel). A schematic diagram of the positions of primers used for H3K4me3 is shown. Specific DNA retrieval was measured by normalization to the amount of input DNA and ChIP signal at GAPDH loci.

(C) ChIP-qPCR analysis of H3K4me3 at the *Ifng* locus in CD8$^+$ T cells from B10.S and B10.S.NeST$^{SJL/J}$ transgenic mice. CD8$^+$ T cells were isolated from four B10.S and four B10.S.NeST$^{SJL/J}$ mice, and stimulated ex vivo with PMA and ionomycin. Occupancy of H3K4me3 at the *Ifng* gene was assayed 24 hr after stimulation by ChIP-qPCR at four different regions. For all pooled data, means and SE are shown.

as possible in the context of individual immunological and other environmental experiences.

EXPERIMENTAL PROCEDURES

Viral and Bacterial Strains and Culture

The DA strain of Theiler's virus was produced by transfecting the PTM762 plasmid into BHK-21 cells as previously described (McAllister et al., 1989). *Salmonella enterica* serovar Typhimurium SL1344 (Subbaiah and Stocker, 1964) strain was used. See Extended Experimental Procedures for inoculation details.

Mouse Strains and Transgenic Line Design

Congenic B10.S.Tmevp3$^{SJL/J}$ and SJL/J.Tmevp3$^{B10.S}$ mice were imported from the Pasteur Institute. B10.S and SJL/J mice were obtained from the Jackson Laboratory (Bar Harbor, ME). (Balb/c x 129) F1 pseudopregnant female mice were provided by Drs. Hugh McDevitt and Grete Sonderstrup (Stanford, CA). All mice were bred at the Stanford Research Animal Facility (RAF) except for the SJLJ/J mice, which were purchased at 4 weeks of age and housed in the Stanford RAF for at least 6 weeks prior to all experiments.

B10.S mice that express NeST RNA transgenically were developed by pronuclear microinjections. NeST cDNA was cloned downstream of a CD4$^+$ and CD8$^+$ T cell-specific promoter and upstream of an SV40 polyadenylation signal (Sawada et al., 1994). Determination of estrous cycle, recovery of single-cell embryos, microinjection procedures, and transfer to pseudopregnant females were performed as previously described (Singer et al., 1998).

Cell Culture, Infection, and Stimulation

Macrophage culture and infection were performed as previously described (Arpaia et al., 2011; Martinat et al., 2002). For T cell culture ex vivo, splenocytes were prepared and CD3$^+$ T cell, CD4$^+$ T cell, or CD8$^+$ T were isolated with the use of kits from Miltenyi Biotec (Auburn, CA). Nuclei were enriched as previously described (Huarte et al., 2010). For T cell stimulation assays, cells were cultured for 10 hr prior to stimulation with 50 ng/ml PMA and 1.5 μM ionomycin (Sigma-Aldrich, St. Louis, MO).

WDR5 and Chromatin IP

NeST$^{B10.S}$, NeST$^{SJL/J}$, HOTTIP, HOTAIR, and U1-encoding cDNAs were cloned into a eukaryotic gene expression plasmid and cotransfected with pcDNA3.1 that did or did not express FlagWDR5. Cells were lysed and immunoprecipitated as previously described, with modifications (Wang et al., 2011). Chromatin IP (ChIP) and qPCR were carried out according to the Farnham protocol (O'Geen et al., 2011).

RNA and Cytokine Quantitation

Protein quantitation was performed using commercially available ELISA kits (R&D Systems, Minneapolis, MN) or Luminex (Affymetrix, Santa Clara, CA) according to the manufacturer's instructions. qRT-PCR was performed with total RNA from cells or tissues of interest and serial dilutions of known quantities of RNA. The three B10.S and 19 SJL/J polymorphisms (Table S1) were introduced by site-directed mutagenesis.

Statistical Analysis

Mean values and significance were determined using Student's t test. Survival curves were analyzed with the log rank test. The null hypothesis (that the strains compared were not different) was rejected when p values were ≤ 0.05. Instances when the observed differences could be reported with a confidence of 95% (*), 99% (**), or 99.9% (***) are denoted.

Additional methods are described in Extended Experimental Procedures.

SUPPLEMENTAL INFORMATION

Supplemental Information includes Extended Experimental Procedures, two figures, and one table and can be found with this article online at http://dx.doi.org/10.1016/j.cell.2013.01.015.

ACKNOWLEDGMENTS

We thank Holden Maecker, Roberto Mateo, and Peter Sarnow for comments on the manuscript. We also thank Laura Attardi for experimental advice, Nigel Killeen for plasmids, Mary Vadeboncoeur and Grete Sonderstrup for their transgenics expertise, Shyamalia Roy for *Salmonella* titering and the Human Immune Monitoring Core for Luminex assays. Individuals involved in this work were supported by scholarships from the Gates Foundation and the Stanford University DARE program (J.A.G.), the National Science Foundation (O.L.W.), the Stanford Medical Science Training Program (Y.W.Y.), and an NIH Training Grant (S.G.). H.Y.C. is an Early Career Scientist of the Howard Hughes Medical Institute. Research funding was provided by the National Society for Multiple Sclerosis (K.K. and M.B.), the Scleroderma Research Foundation (H.Y.C.), and an NIH Director's Pioneer Award (K.K.).

Received: March 1, 2012
Revised: July 28, 2012
Accepted: January 7, 2013
Published: February 14, 2013

REFERENCES

Arpaia, N., Godec, J., Lau, L., Sivick, K.E., McLaughlin, L.M., Jones, M.B., Dracheva, T., Peterson, S.N., Monack, D.M., and Barton, G.M. (2011). TLR signaling is required for Salmonella typhimurium virulence. Cell *144*, 675–688.

Aubagnac, S., Brahic, M., and Bureau, J.F. (2002). Bone marrow chimeras reveal non-H-2 hematopoietic control of susceptibility to Theiler's virus persistent infection. J. Virol. *76*, 5807–5812.

Balasubramani, A., Mukasa, R., Hatton, R.D., and Weaver, C.T. (2010). Regulation of the Ifng locus in the context of T-lineage specification and plasticity. Immunol. Rev. *238*, 216–232.

Bihl, F., Brahic, M., and Bureau, J.F. (1999). Two loci, Tmevp2 and Tmevp3, located on the telomeric region of chromosome 10, control the persistence of Theiler's virus in the central nervous system of mice. Genetics *152*, 385–392.

Brahic, M., Bureau, J.F., and Michiels, T. (2005). The genetics of the persistent infection and demyelinating disease caused by Theiler's virus. Annu. Rev. Microbiol. *59*, 279–298.

Broz, P., Newton, K., Lamkanfi, M., Mariathasan, S., Dixit, V.M., and Monack, D.M. (2010). Redundant roles for inflammasome receptors NLRP3 and NLRC4 in host defense against Salmonella. J. Exp. Med. *207*, 1745–1755.

Bureau, J.F., Montagutelli, X., Lefebvre, S., Guénet, J.L., Pla, M., and Brahic, M. (1992). The interaction of two groups of murine genes determines the persistence of Theiler's virus in the central nervous system. J. Virol. *66*, 4698–4704.

Bureau, J.F., Montagutelli, X., Bihl, F., Lefebvre, S., Guénet, J.L., and Brahic, M. (1993). Mapping loci influencing the persistence of Theiler's virus in the murine central nervous system. Nat. Genet. *5*, 87–91.

Cagliani, R., Riva, S., Pozzoli, U., Fumagalli, M., Comi, G.P., Bresolin, N., Clerici, M., and Sironi, M. (2011). Balancing selection is common in the extended MHC region but most alleles with opposite risk profile for autoimmune diseases are neutrally evolving. BMC Evol. Biol. *11*, 171.

Chang, B., Mandal, M.N., Chavali, V.R., Hawes, N.L., Khan, N.W., Hurd, R.E., Smith, R.S., Davisson, M.L., Kopplin, L., Klein, B.E., et al. (2008). Age-related retinal degeneration (arrd2) in a novel mouse model due to a nonsense mutation in the Mdm1 gene. Hum. Mol. Genet. *17*, 3929–3941.

Chang, S., and Aune, T.M. (2005). Histone hyperacetylated domains across the Ifng gene region in natural killer cells and T cells. Proc. Natl. Acad. Sci. USA *102*, 17095–17100.

Chu, C., Qu, K., Zhong, F.L., Artandi, S.E., and Chang, H.Y. (2011). Genomic maps of long noncoding RNA occupancy reveal principles of RNA-chromatin interactions. Mol. Cell *44*, 667–678.

Collier, S.P., Collins, P.L., Williams, C.L., Boothby, M.R., and Aune, T.M. (2012). Cutting edge: influence of Tmevpg1, a long intergenic noncoding RNA, on the expression of Ifng by Th1 cells. J. Immunol. *189*, 2084–2088.

Davila, E., Kang, Y.M., Park, Y.W., Sawai, H., He, X., Pryshchep, S., Goronzy, J.J., and Weyand, C.M. (2005). Cell-based immunotherapy with suppressor CD8+ T cells in rheumatoid arthritis. J. Immunol. *174*, 7292–7301.

Dean, M., Carrington, M., and O'Brien, S.J. (2002). Balanced polymorphism selected by genetic versus infectious human disease. Annu. Rev. Genomics Hum. Genet. *3*, 263–292.

Foster, N., Hulme, S.D., and Barrow, P.A. (2005). Inhibition of IFN-gamma-stimulated proinflammatory cytokines by vasoactive intestinal peptide (VIP) correlates with increased survival of Salmonella enterica serovar typhimurium phoP in murine macrophages. J. Interferon Cytokine Res. *25*, 31–42.

Frehel, C., Canonne-Hergaux, F., Gros, P., and De Chastellier, C. (2002). Effect of Nramp1 on bacterial replication and on maturation of Mycobacterium avium-containing phagosomes in bone marrow-derived mouse macrophages. Cell. Microbiol. *4*, 541–556.

Frisullo, G., Nociti, V., Iorio, R., Plantone, D., Patanella, A.K., Tonali, P.A., and Batocchi, A.P. (2010). CD8(+)Foxp3(+) T cells in peripheral blood of relapsing-remitting multiple sclerosis patients. Hum. Immunol. *71*, 437–441.

Goris, A., Heggarty, S., Marrosu, M.G., Graham, C., Billiau, A., and Vandenbroeck, K. (2002). Linkage disequilibrium analysis of chromosome 12q14-15 in multiple sclerosis: delineation of a 118-kb interval around interferon-gamma (IFNG) that is involved in male versus female differential susceptibility. Genes Immun. *3*, 470–476.

Guttman, M., and Rinn, J.L. (2012). Modular regulatory principles of large non-coding RNAs. Nature *482*, 339–346.

Guttman, M., Amit, I., Garber, M., French, C., Lin, M.F., Feldser, D., Huarte, M., Zuk, O., Carey, B.W., Cassady, J.P., et al. (2009). Chromatin signature reveals over a thousand highly conserved large non-coding RNAs in mammals. Nature *458*, 223–227.

Hadjur, S., Williams, L.M., Ryan, N.K., Cobb, B.S., Sexton, T., Fraser, P., Fisher, A.G., and Merkenschlager, M. (2009). Cohesins form chromosomal cis-interactions at the developmentally regulated IFNG locus. Nature *460*, 410–413.

Huarte, M., Guttman, M., Feldser, D., Garber, M., Koziol, M.J., Kenzelmann-Broz, D., Khalil, A.M., Zuk, O., Amit, I., Rabani, M., et al. (2010). A large intergenic noncoding RNA induced by p53 mediates global gene repression in the p53 response. Cell *142*, 409–419.

Jeon, Y., and Lee, J.T. (2011). YY1 tethers Xist RNA to the inactive X nucleation center. Cell *146*, 119–133.

Joosten, S.A., van Meijgaarden, K.E., Savage, N.D., de Boer, T., Triebel, F., van der Wal, A., de Heer, E., Klein, M.R., Geluk, A., and Ottenhoff, T.H. (2007). Identification of a human CD8+ regulatory T cell subset that mediates suppression through the chemokine CC chemokine ligand 4. Proc. Natl. Acad. Sci. USA *104*, 8029–8034.

Khalil, A.M., Guttman, M., Huarte, M., Garber, M., Raj, A., Rivea Morales, D., Thomas, K., Presser, A., Bernstein, B.E., van Oudenaarden, A., et al. (2009). Many human large intergenic noncoding RNAs associate with chromatin-modifying complexes and affect gene expression. Proc. Natl. Acad. Sci. USA *106*, 11667–11672.

Latiano, A., Palmieri, O., Latiano, T., Corritore, G., Bossa, F., Martino, G., Biscaglia, G., Scimeca, D., Valvano, M.R., Pastore, M., et al. (2011). Investigation of multiple susceptibility loci for inflammatory bowel disease in an Italian cohort of patients. PLoS ONE *6*, e22688.

Levillayer, F., Mas, M., Levi-Acobas, F., Brahic, M., and Bureau, J.F. (2007). Interleukin 22 is a candidate gene for Tmevp3, a locus controlling Theiler's virus-induced neurological diseases. Genetics *176*, 1835–1844.

Libioulle, C., Louis, E., Hansoul, S., Sandor, C., Farnir, F., Franchimont, D., Vermeire, S., Dewit, O., de Vos, M., Dixon, A., et al. (2007). Novel Crohn disease locus identified by genome-wide association maps to a gene desert on 5p13.1 and modulates expression of PTGER4. PLoS Genet. *3*, e58.

Liu, R., Paxton, W.A., Choe, S., Ceradini, D., Martin, S.R., Horuk, R., MacDonald, M.E., Stuhlmann, H., Koup, R.A., and Landau, N.R. (1996). Homozygous defect in HIV-1 coreceptor accounts for resistance of some multiply-exposed individuals to HIV-1 infection. Cell *86*, 367–377.

Martinat, C., Mena, I., and Brahic, M. (2002). Theiler's virus infection of primary cultures of bone marrow-derived monocytes/macrophages. J. Virol. *76*, 12823–12833.

McAllister, A., Tangy, F., Aubert, C., and Brahic, M. (1989). Molecular cloning of the complete genome of Theiler's virus, strain DA, and production of infectious transcripts. Microb. Pathog. *7*, 381–388.

Miao, E.A., and Rajan, J.V. (2011). Salmonella and Caspase-1: a complex interplay of detection and evasion. Front. Microbiol. *2*, 85.

Monack, D.M., Bouley, D.M., and Falkow, S. (2004). Salmonella typhimurium persists within macrophages in the mesenteric lymph nodes of chronically infected Nramp1+/+ mice and can be reactivated by IFNgamma neutralization. J. Exp. Med. *199*, 231–241.

Nagano, T., Mitchell, J.A., Sanz, L.A., Pauler, F.M., Ferguson-Smith, A.C., Feil, R., and Fraser, P. (2008). The Air noncoding RNA epigenetically silences transcription by targeting G9a to chromatin. Science *322*, 1717–1720.

O'Geen, H., Echipare, L., and Farnham, P.J. (2011). Using ChIP-seq technology to generate high-resolution profiles of histone modifications. Methods Mol. Biol. *791*, 265–286.

Ong, C.T., and Corces, V.G. (2011). Enhancer function: new insights into the regulation of tissue-specific gene expression. Nat. Rev. Genet. *12*, 283–293.

Ørom, U.A., Derrien, T., Beringer, M., Gumireddy, K., Gardini, A., Bussotti, G., Lai, F., Zytnicki, M., Notredame, C., Huang, Q., et al. (2010). Long noncoding RNAs with enhancer-like function in human cells. Cell *143*, 46–58.

Orozco, G., Eerligh, P., Sánchez, E., Zhernakova, S., Roep, B.O., González-Gay, M.A., López-Nevot, M.A., Callejas, J.L., Hidalgo, C., Pascual-Salcedo, D., et al. (2005). Analysis of a functional BTNL2 polymorphism in type 1 diabetes, rheumatoid arthritis, and systemic lupus erythematosus. Hum. Immunol. *66*, 1235–1241.

Rossi, C.P., Delcroix, M., Huitinga, I., McAllister, A., van Rooijen, N., Claassen, E., and Brahic, M. (1997). Role of macrophages during Theiler's virus infection. J. Virol. *71*, 3336–3340.

Pereira, M.S., Marques, G.G., Dellama, J.E., and Zamboni, D.S. (2011). The Nlrc4 inflammasome contributes to restriction of pulmonary infection by flagellated Legionella spp. that trigger pyroptosis. Front. Microbiol. *2*, 33.

Qureshi, I.A., Mattick, J.S., and Mehler, M.F. (2010). Long non-coding RNAs in nervous system function and disease. Brain Res. *1338*, 20–35.

Rodriguez, M., Zoecklein, L.J., Howe, C.L., Pavelko, K.D., Gamez, J.D., Nakane, S., and Papke, L.M. (2003). Gamma interferon is critical for neuronal viral clearance and protection in a susceptible mouse strain following early intracranial Theiler's murine encephalomyelitis virus infection. J. Virol. *77*, 12252–12265.

Sawada, S., Scarborough, J.D., Killeen, N., and Littman, D.R. (1994). A lineage-specific transcriptional silencer regulates CD4 gene expression during T lymphocyte development. Cell *77*, 917–929.

Sekimata, M., Pérez-Melgosa, M., Miller, S.A., Weinmann, A.S., Sabo, P.J., Sandstrom, R., Dorschner, M.O., Stamatoyannopoulos, J.A., and Wilson, C.B. (2009). CCCTC-binding factor and the transcription factor T-bet orchestrate T helper 1 cell-specific structure and function at the interferon-gamma locus. Immunity *31*, 551–564.

Silverberg, M.S., Cho, J.H., Rioux, J.D., McGovern, D.P., Wu, J., Annese, V., Achkar, J.P., Goyette, P., Scott, R., Xu, W., et al. (2009). Ulcerative colitis-risk loci on chromosomes 1p36 and 12q15 found by genome-wide association study. Nat. Genet. *41*, 216–220.

Singer, S.M., Tisch, R., Yang, X.D., Sytwu, H.K., Liblau, R., and McDevitt, H.O. (1998). Prevention of diabetes in NOD mice by a mutated I-Ab transgene. Diabetes *47*, 1570–1577.

Sirota, M., Schaub, M.A., Batzoglou, S., Robinson, W.H., and Butte, A.J. (2009). Autoimmune disease classification by inverse association with SNP alleles. PLoS Genet. *5*, e1000792.

Sotelo, J., Esposito, D., Duhagon, M.A., Banfield, K., Mehalko, J., Liao, H., Stephens, R.M., Harris, T.J., Munroe, D.J., and Wu, X. (2010). Long-range enhancers on 8q24 regulate c-Myc. Proc. Natl. Acad. Sci. USA *107*, 3001–3005.

Strowig, T., Henao-Mejia, J., Elinav, E., and Flavell, R. (2012). Inflammasomes in health and disease. Nature *481*, 278–286.

Subbaiah, T.V., and Stocker, B.A. (1964). Rough mutants of Salmonella Typhimurium. I. Genetics. Nature *201*, 1298–1299.

Sun, J., Madan, R., Karp, C.L., and Braciale, T.J. (2009). Effector T cells control lung inflammation during acute influenza virus infection by producing IL-10. Nat. Med. *15*, 277–284.

Tian, D., Sun, S., and Lee, J.T. (2010). The long noncoding RNA, Jpx, is a molecular switch for X chromosome inactivation. Cell *143*, 390–403.

Trandem, K., Zhao, J., Fleming, E., and Perlman, S. (2011). Highly activated cytotoxic CD8 T cells express protective IL-10 at the peak of coronavirus-induced encephalitis. J. Immunol. *186*, 3642–3652.

Valentonyte, R., Hampe, J., Huse, K., Rosenstiel, P., Albrecht, M., Stenzel, A., Nagy, M., Gaede, K.I., Franke, A., Haesler, R., et al. (2005). Sarcoidosis is associated with a truncating splice site mutation in BTNL2. Nat. Genet. *37*, 357–364.

Vigneau, S., Levillayer, F., Crespeau, H., Cattolico, L., Caudron, B., Bihl, F., Robert, C., Brahic, M., Weissenbach, J., and Bureau, J.F. (2001). Homology between a 173-kb region from mouse chromosome 10, telomeric to the Ifng locus, and human chromosome 12q15. Genomics *78*, 206–213.

Vigneau, S., Rohrlich, P.S., Brahic, M., and Bureau, J.F. (2003). Tmevpg1, a candidate gene for the control of Theiler's virus persistence, could be implicated in the regulation of gamma interferon. J. Virol. *77*, 5632–5638.

Wang, K., Baldassano, R., Zhang, H., Qu, H.Q., Imielinski, M., Kugathasan, S., Annese, V., Dubinsky, M., Rotter, J.I., Russell, R.K., et al. (2010). Comparative genetic analysis of inflammatory bowel disease and type 1 diabetes implicates multiple loci with opposite effects. Hum. Mol. Genet. *19*, 2059–2067.

Wang, K.C., and Chang, H.Y. (2011). Molecular mechanisms of long noncoding RNAs. Mol. Cell *43*, 904–914.

Wang, K.C., Yang, Y.W., Liu, B., Sanyal, A., Corces-Zimmerman, R., Chen, Y., Lajoie, B.R., Protacio, A., Flynn, R.A., Gupta, R.A., et al. (2011). A long

noncoding RNA maintains active chromatin to coordinate homeotic gene expression. Nature *472*, 120–124.

Williams, T.N., Mwangi, T.W., Wambua, S., Peto, T.E., Weatherall, D.J., Gupta, S., Recker, M., Penman, B.S., Uyoga, S., Macharia, A., et al. (2005). Negative epistasis between the malaria-protective effects of alpha+-thalassemia and the sickle cell trait. Nat. Genet. *37*, 1253–1257.

Xystrakis, E., Dejean, A.S., Bernard, I., Druet, P., Liblau, R., Gonzalez-Dunia, D., and Saoudi, A. (2004). Identification of a novel natural regulatory CD8 T-cell subset and analysis of its mechanism of regulation. Blood *104*, 3294–3301.

Zhou, W., Chang, S., and Aune, T.M. (2004). Long-range histone acetylation of the Ifng gene is an essential feature of T cell differentiation. Proc. Natl. Acad. Sci. USA *101*, 2440–2445.